

A Study of the Relation Between Nozzle Geometry, Internal flow and Sprays Characteristics in Diesel Fuel Injection Systems

Raul Payri*, S. Molina, F. J. Salvador, J. Gimeno
CMT-Motores Termicos, Universidad Polit cnica de Valencia
Camino de Vera s/n, E-46022 Spain

This study examines the influence of geometry on the internal flow and macroscopic behavior of the spray in Diesel nozzles. For this investigation, two bi-orifice nozzles were employed : one cylindrical and one conical. The first step is to use a non-destructive characterization method which is based on the production of silicone moulds so that the precise internal geometry of the two nozzles can be measured. At this stage the nozzles have been characterized dimensionally and therefore the internal flow can be studied using CFD calculations. The results gained from this experiment make it possible also to ascertain the critical cavitation conditions. Once the critical cavitation conditions have been identified, the macroscopic parameters of the spray can be studied in both cavitating and non-cavitating conditions using a test rig pressurized with nitrogen and with the help of a image acquisition system and image processing software. Consequently, research can be carried out to determine the influence that cavitation has on macroscopic spray behavior. From the point of view of the spray macroscopic behavior, the main conclusion of the paper is that cavitation leads to an increment of the spray cone angle. On the other hand, from the point of view of the internal flow, the hole outlet velocity increases when cavitation appears. This phenomenon can be explained by the reduction in the cross section of the liquid phase in the outlet section of the hole.

Key Words : CFD, Nozzle Flow, Spray, Cavitation, Diesel Injection, Nozzle Geometry

Nomenclature

A : Total surface of the nozzle orifice at the outlet	D_m : Diameter at the middle of the orifice
A_o : Surface of one orifice at the outlet	D_o : Diameter at the orifice outlet
AR : Area reduction of the nozzle orifices	F : Coefficient of the discharge coefficient regression
C_a : Contraction coefficient at the orifice outlet	G : Coefficient of the discharge coefficient regression
C_c : Nurick contraction coefficient	\dot{m} : Mass flow rate of the nozzle
C_d : Discharge coefficient	\dot{m}_o : Mass flow rate of one orifice of the nozzle
C_v : Velocity coefficient at the orifice outlet	M_o : Momentum flux at the orifice outlet
CN : Cavitation Number	P_i : Injection pressure
D_{eq} : Equivalent diameter	P_b : Downstream pressure (backpressure)
D_i : Diameter at the orifice inlet	P_v : Vaporisation pressure
	R_a : Upper rounding radius at the inlet orifice
	R_b : Lower rounding radius at the inlet orifice
	Re : Reynolds number
	S : Spray penetration
	t : Time
	U_o : Velocity at the orifice outlet
	U_{th} : Theoretical velocity.

* Corresponding Author,

E-mail : rpayri@mot.upv.es

TEL : +34-963879658; **FAX :** +34-963877659

CMT-Motores Termicos, Universidad Polit cnica de Valencia Camino de Vera s/n, E-46022 Spain. (Manuscript Received November 20, 2003; Revised April 12, 2004)

Greek symbols

- P : Pressure differential, $\Delta P = P_i - P_b$
 ρ : Gasoil density
 ρ_a : Air density
 θ : Spray cone angle.
 $\theta/2$: Spray cone semi-angle
 μ : Dynamic viscosity
 ν : Kinematic viscosity

Subscripts

crit: Cavitation critical conditions

1. Introduction

The injector nozzle is one of the most important parts of a Diesel engine. Nozzle geometry affects spray characteristics and therefore atomization behavior, which is decisive for engine performance and pollutant formation. A major objective of the research carried out in this area in the past few years has been to improve nozzle design in order to obtain better air fuel mixing. A thorough understanding of the internal flow physics inside the nozzle is fundamental for predicting spray development. There is experimental evidence to show that cavitation within the nozzle modifies the characteristics of the nozzle exit spray and probably favors atomization of the spray (He and Ruiz, 1995; Soteriou et al., 1995). It may, however, also affect the internal flow in other ways that are not yet clear. Real size production nozzles have very small dimensions and operate at very high injection pressure over very short time periods. It is therefore very difficult to visualize the internal flow. Hence, most of these studies were performed on large-scale transparent models (Arcoumanis et al., 1999; Ganippa et al., 2001; He and Ruiz, 1995; Soteriou et al., 1995) with the aim of visualizing the cavitation structure within the nozzles. Different types of nozzles have been investigated, from one-orifice nozzles in references (Arcoumanis et al., 1999; He and Ruiz, 1995) to different multi-hole VCO and Sac-nozzles. The same authors have also studied the velocity field using the LDV technique. Real size nozzle studies were also performed by several authors (Arcoumanis et al., 1998; 2000; Badock

et al., 1997; 1999; Chaves et al., 1995). In particular, Arcoumanis et al. (2000) observed that the cavitation structure was different in large scale and real size experiments.

Owing to the difficulties associated with the determination of flow characteristics inside a Diesel Nozzle, CFD calculations represent a very useful tool to provide an insight into the three dimensional flow inside the nozzle. Various attempts were made to predict cavitation flow numerically. (Bunnell and Heister, 2000; Schmidt et al., 1999) Throughout the past few years, studies have been carried out looking at the influence of nozzle geometries on the fuel spray behavior and performance features of the engine, independently from the study of cavitation (Choi et al., 2002; Kampmann et al., 1996; Koo, 2003; Ohn et al., 1991; Pierpont and Reitz, 1995). However, it is not clear whether the discrepancies found in the results are wholly due to the differences in nozzle geometries, or are in part due to the existence or non-existence of cavitation.

With respect to the influence of cavitation on the spray, there is a bibliography of several studies that have concentrated on highlighting the connection between cavitation and the previous development of the spray (Badock et al., 1997; 1999; Bergwerk, 1959; Blessing et al., 2003; Chaves et al., 1995; Lee et al., 2002; Soteriou et al., 1995) For example, Chaves et al. (1995) detected within their studies of spray visualization, an enlargement of the spray cone angle when cavitation started.

In this paper, a study was carried out examining the influence of cavitation on the internal flow and the macroscopic behavior of the spray. For the study, the nozzles chosen were two bi-orifices: one of which has cylindrical orifices and small values for the radii of curvature at the orifice entrance and the other which has orifices with large conicity and thus a large radii of curvature at the orifice inlet. Previous studies show that an increase in the conicity and radii of curvature reduces the likelihood of cavitation in the nozzle (Badock et al., 1999; Ohn et al., 1991; Macián et al., 2003b; Nurick, 1976; Payri et al., 2002).

When looking at cavitation, the two chosen nozzles are very different, as the first nozzle is much more inclined to cavitate, whereas the second nozzle inhibits the cavitation phenomenon, as studied by Payri et al. (2002). Firstly, the internal geometries of both nozzles were determined. In order to do this, a non-destructive characterization method was used which is based on the creation of silicone moulds and then follows the methodology explained by Macián et al. (2003a). This technique makes it possible to determine the orifices' diameter values and the conicity. It is also possible to obtain values of the radii of the rounded orifice entrances and any other internal geometrical irregularities. This characterization is necessary because, even though qualitatively the nozzles are manufactured in such a way that the values for conicity are given, as are the according radii, the final values for these parameters depend on the process of hydro-grinding applied in the final process of manufacturing (Kampmann et al., 1996; Potz et al., 2000).

Once the nozzles have been characterized dimensionally, an examination of the internal flow follows using CFD calculations. The critical cavitation conditions are determined numerically to detect which pressure conditions lead the pressure in the nozzle to diminish to the value of the vapor pressure (Macián et al., 2003b).

The identification of the critical cavitation conditions makes it possible to carry out a study on the macroscopic parameters of the spray, in cavitating and non-cavitating conditions, and therefore enables the influence of the phenomenon on the macroscopic behavior of the spray to be determined. For this spray macroscopic study, a high-pressure nitrogen test rig was used in order to visualize the sprays for density conditions which are similar to the real conditions in the engine. With the help of an image acquisition system, as well as image processing software, images taken can be processed using a segmentation algorithm based on the log-likelihood ratio test (Pastor et al., 2001). Lastly, a theoretical analysis of the results makes it possible to establish the influence the cavitation phenomenon has on flow parameters such as the velocity coefficient

and contraction coefficient, which further facilitates the study of the influence on the process of air-fuel mixing.

2. Experimental Facilities

This section provides a brief description of the experimental facilities used for the studies presented in this paper. The fuel injection system is a standard common rail (Flaig et al., 1999) with a high-pressure pump able to reach up to 1350 bar and a conventional rail with a pressure regulator.

The experimental facilities are as follows:

- (1) Determination of the internal geometry.
- (2) The Nitrogen test rig.
- (3) Image acquisition system and image processing software.

These experimental tools are described below.

2.1 Determination of the internal geometry

In order to analyze the internal geometrical characteristics of the nozzles, a particular methodology was followed (Macián et al., 2003a). This methodology is based on the use of a special type of silicone to obtain the internal moulds of the nozzle. Once the moulds have been obtained, pictures of the moulds are taken with a microscope. The characteristic dimensions are calculated from the pictures using computer-aided design (CAD) software. With respect to other methods it has the advantage of being able to obtain all

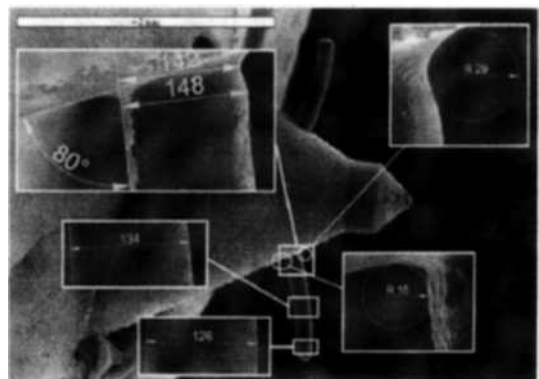


Fig. 1 Dimensional characterization of the convergent nozzle

the dimensions of non-optical accessible parts of the nozzles and is also non-destructive. This experimental tool is useful for the study of Diesel sprays, because it enables researchers to establish relationships between internal geometry, internal flow (Payri et al., 2002) and spray characteristics.

Figure 1 shows the photos taken of the conical nozzle, from which the diameters at the inlet, middle and outlet have been measured. They also show the upper and lower rounding radii.

2.2 Nitrogen test rig

In order to visualize the sprays, the nitrogen test rig is used. The test rig basically consists of a steel cube with a chamber and various connecting flanges machined into it. The design is modular, and ancillaries can be added depending on the required experiment (Pastor et al., 2003). The test rig is designed for a maximum pressure of 80 bar. The test rig has an internal volume of 1 liter.

The nitrogen must be circulated through the rig because otherwise the injected Diesel will obscure the windows and severely degrade the quality of the images. Furthermore, it is important to keep rig pressure (P_b) and nitrogen temperature constant during each experiment. Two filters collect the injected fuel to keep the gas stream clean. The temperature of the nitrogen can be fixed between 15 and 50°C in order to obtain the desired density inside the chamber. The test rig operates at all times in cold conditions thus avoiding fuel evaporation.

2.3 Image acquisition system and image processing software

The images are taken with a 12-bit colour CCD camera with a spatial resolution of 1280 × 1024 pixels, a minimum exposure time of 10 microseconds with a jitter of ±5 microseconds. Illumination is created with a conventional electronic flash, with controllable duration (set for far longer than the minimum camera gate) and intensity. Despite this type of conventional flash used to present a shot-to-shot fluctuation that is higher than more sophisticated light sources,

the results obtained with the software have proved to be insensitive to fluctuations in the illumination intensity within a reasonable range. All the experimental equipment (camera-flash-injection) has been synchronized with a purpose-built electronic system, using the injector trigger signal as a reference signal to take the image sequences. The relative position between the camera and the flash depends on the type of visualization technique. In this study, the visualization of the sprays is carried out using the shadowgraphy technique. In order to avoid obscuring the windows, nozzles with two orifices were used. The injector is positioned so that the sprays are situated perpendicular to the camera and flash window. This also allows a characterization of each spray to be made without interferences from others. Figure 2 (upper part and left) shows the relative position of the flash, camera and injector, with the camera placed in the window at the front, and the flash in the window at the back. The injector is placed in the middle of them. Figure 2 (right) shows one sample of an image of a spray taken using this technique. The injection is controlled with a purpose-built ECU system that allows injection to take place at a very low frequency (0.25 Hz). This very low frequency is needed in order to avoid window dirt in the injection chamber.

The images are digitally processed using purpose-developed software (Pastor et al., 2001). The segmentation algorithm used, based on the log-likelihood ratio test (LRT), has the advantage of using the three channels of RGB images

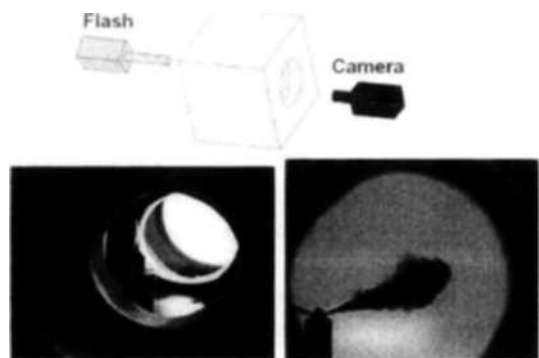


Fig. 2 Relative position of the flash, camera and injector. Sample of an image of a spray

for a proper determination of boundaries that are not clearly defined, as in the case of sprays. This method proved to be almost completely insensitive to intensity fluctuations between pictures for the tested cases, and provided better results than some other algorithms checked. Prior to the systematic use of the algorithm for parametric studies, the influence of the illumination quality on the results was evaluated in specific tests. Results demonstrated that the algorithm properly detects the estimated spray boundaries even in the case of reasonably poor illumination. Details of the image processing software are available in (Pastor et al., 2001).

3. The CFD Approach

In order to explore the characteristics of the nozzle's internal flow, a numerical study was carried out. The aim of this study was to compare both nozzles in terms of internal nozzle flow characteristics in non-cavitating conditions and to compare the critical pressure conditions that induces the nozzles to cavitate.

The numerical study presented in this article was made with a finite volume flow program Fluent (2001). This code has been used to solve the discretized Navier-Stokes equations (Versteeg et al., 1995). The program is based on the pressure correction method and uses the SIMPLE algorithm (Versteeg et al., 1995). The first order Upwind Differencing scheme is used for the momentum equation. Preliminary CFD Diesel nozzle calculations presented in previous work (Macián et al., 2003b) made it possible to choose the appropriate mesh fineness for the calculations foreseen, as well as the most adequate turbulence model. All calculations presented here are made using the standard $k-\varepsilon$ turbulence model with standard wall functions.

Constant pressure boundary conditions were assigned at the nozzle entrance and exit boundaries, with an injection pressure of 30 MPa, and a backpressure of 6 MPa.

The steady-state calculations presented in this section are for the 3D nozzle geometries, reproductions of those obtained from the silicone

methodology, and simulating the needle in the maximum position. Three-dimensional effects due to the sudden change in flow direction at the orifice entrance and to possible asymmetries of the nozzle geometry are thus considered.

Typical liquid gasoil (C16H29) fluid properties were considered throughout the study, i.e. the density, dynamic viscosity and vapor pressure are respectively :

$$\rho=820 \text{ Kg/m}^3$$

$$\mu=3.32 \cdot 10^{-3} \text{ kg/(m.s)}$$

$$P_v=0.08 \text{ MPa}$$

The convergence criteria used for the calculations were two-fold : on the one hand, residuals for all equations had to have reached a value at least of 10^{-3} , on the other hand, the average velocity profile at the exit had to be stabilized. Solutions could thus be obtained within reasonable calculation time.

4. Results

4.1 Nozzle geometry determination

Using the silicone technique, the two nozzle moulds have been obtained.

Two valve-covered orifices (VCO) nozzles with two orifices were used. As explained in Macián et al.(2003a), a scanning electron microscope is used to obtain the images. The pictures obtained with the electronic microscope come with a reference dimension (magnification factor) as shown in Fig. 1. With this information the pictures can be loaded in the computer-aided design software with the appropriate scale factor. Since the exact magnification factor is used, it is not difficult to obtain the actual dimensions of the nozzle.

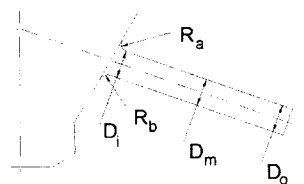


Fig. 3 Nozzle hole parameters that can be characterized with the silicone methodology

Table 1 Dimensions of the cylindrical nozzle

Orifice	R_a	R_b	D_i	D_m	D_o	AR [%]
1	8	12	133	131	131	3
2	7	13	133	130	131	3
Mean	7.5	12.5	133	130.5	131	3

Table 2 Dimensions of the conical nozzle

Orifice	R_a	R_b	D_i	D_m	D_o	AR [%]
1	19	27	143	138	125	23.6
2	15	29	144	134	125	24.6
Mean	17	28	143.5	136	125	24.1

Figure 3 shows a sketch where the nozzle hole parameters that have been measured are depicted. In this figure, R_a and R_b are the upper and lower rounding radii at the inlet orifice and D_i , D_m and D_o , are the diameters of the orifice at the inlet, middle and outlet.

Table 1 and Table 2 show the results obtained for each orifice in the two nozzles tested. In these tables AR is the area reduction (conicity) of the nozzle orifices calculated as :

$$AR = \frac{D_i^2 - D_o^2}{D_i^2} \cdot 100 \quad (1)$$

In the third row the mean values of each parameter are calculated. As can be deduced from the table, there is little dispersion between the two orifices of both nozzles, so the mean parameters could be taken as representative values of the nozzles.

As previously commented, the first nozzle has a small conicity and low values of the rounding radii, so it has a strong tendency to cavitate (Blessing et al., 2003 ; Macián et al., 2003b ; Payri et al., 2002). On the contrary, the second nozzle has a large value of area reduction so it has a high degree of conicity. Also, in comparison with the first, this nozzle has larger values of rounding radii, so in this case cavitation could be reduced, or even eliminated.

4.2 Investigation of the internal flow. Critical cavitation conditions

The purpose of the calculations presented here

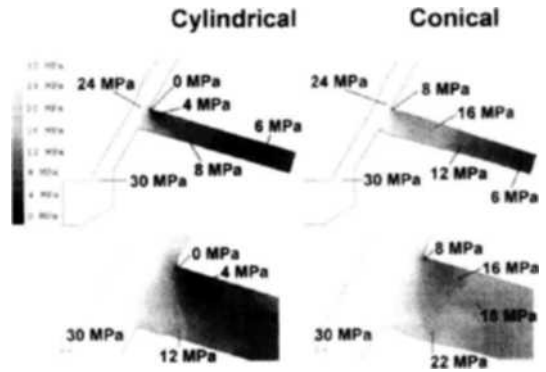


Fig. 4 Pressure field for the cylindrical and conical nozzle. $P_i=30$ MPa, $P_b=6$ MPa

is to compare the behavior of the internal flow of both nozzles with particular attention to the influence of the nozzle geometry on the onset of cavitation. The critical cavitation conditions will be identified, and thus a study of the influence of geometry and cavitation on the macroscopic spray behavior can be performed.

Figure 4 shows the representation of the pressure field for the cylindrical and the conical nozzle. The boundary conditions used are 30 MPa as inlet pressure (P_i) and 6 MPa as discharge pressure (P_b). The backpressure of 6 MPa was selected since this value is representative of real pressure in the engine combustion chamber during the injection process. As may be seen by comparing both contours, the effect of the convergent nozzle is to soften the pressure gradients within the nozzle. This can be explained mainly by the gradual acceleration of the flow in the convergent nozzle due to the conicity ($AR=24\%$ versus $AR=3\%$ in the cylindrical case) and also the less brutal change in flow direction when the flow rounds the upper inlet corner ($R_a=17$ versus $R_a=7.5$). Only the upper rounding radius (and not the lower rounding radius) has to be considered because it directly affects the flow path and as a consequence it is responsible for the pressure drop. For the cylindrical nozzle, the minimum pressure suddenly falls to a minimum value of 0 MPa and it is placed in the upper corner of the inlet orifice. Considering that the vapor pressure is 0.08 MPa, the critical pressure conditions of onset of cavitation are achieved for

the cylindrical nozzle. Nevertheless, the minimum pressure of the convergent nozzle is 6 MPa at the orifice exit, avoiding cavitation phenomenon. Cavitation conditions in an injector can be represented using some of the different cavitation numbers proposed in the literature. These are non-dimensional parameters that make it possible to establish whether or not the relevant flow conditions in the injector nozzle, that is to say, the pressure differential, are favorable to the occurrence of cavitation. Definitions of these parameters vary throughout the literature (Bergwerk, 1959; Macián et al., 2003b; Nurick, 1976; Soteriou et al., 1995) but they are mainly based on the pressure difference across the injector orifice. In this study, the cavitation number definition used by Soteriou et al. (1995) is employed :

$$CN = \frac{P_i - P_b}{P_b - P_v} \quad (2)$$

Where P_v is the vapor pressure.

For cavitating nozzles, the critical cavitation number is defined as CN_{crit} , corresponding to the pressure drop at which cavitation starts in the injector orifice. Hence, cavitation will not occur unless the cavitation number corresponding to these pressure conditions is higher than the critical value (CN_{crit}).

Therefore, considering this definition, for the cylindrical nozzle a critical cavitation number of $CN_{crit} = 4$ is found. This critical cavitation number depends on the geometry and therefore the critical pressure conditions of cavitation ($P_i = 30$ MPa $P_b = 6$ MPa) are only valid for this case. Nevertheless, for the convergent nozzle, even with an injection pressure of 80 MPa, critical cavitation conditions were not reached.

4.3 Influence of geometry on the macroscopic characteristics of the spray

Once the dimensional characterization and the identification of the critical cavitation conditions have been made, this section studies the influence of the cavitation phenomenon on the macroscopic behavior of the spray. With the results obtained, an analysis is made looking at the influence of cavitation on the present mechanisms

in the injection-combustion process.

Visualization studies have been carried out for the two nozzles at different injection pressures. The tested injection pressures, P_i , considered, were between 20 MPa and 80 MPa (14 values were chosen). The pressure inside the visualization test bench, which is therefore equal to the discharge pressure of the injector (P_b), was 6 MPa. With the wide range of tested pressures that are considered, and taking into account the critical cavitation conditions of the cylindrical nozzle, it is possible to characterize the spray under conditions that are distinctly non-cavitating and cavitating.

Higher variations of injection pressure were considered for the cylindrical nozzle to study the influence of cavitation on the macroscopic parameters of the spray. Furthermore, working at elevated contra-pressures makes it possible to approximate the real conditions that exist in the combustion chamber of the engine. The energizing time of the injector was set at 2000 μ s, and the test bench temperature has been regulated and maintained at a constant value of 30°C.

Under these conditions, and in order to take images of the sprays during the whole injection process, the characterization temporary interval was chosen from 200 μ s to 3000 μ s. These time periods are measured from the start of the electrical excitation of the injector. The value of 200 μ s generally corresponds (depending on the injection pressure) to the instant when the spray starts to appear, whilst the value of 3000 μ s corresponds to a completely developed spray for the value of the considered pulse. Within this range, the images were taken every 100 μ s during the injection process, which means a total of 31 instants were measured during the process. For each of these instants, 10 repetitions were carried out, and values of the measured macroscopic parameters were obtained using the image treatment program.

Before the presentation and analysis of results it is necessary to determine the objectives of the visualization study. For the tested injection pressure, and taking into account that the discharge pressure is maintained at a constant value

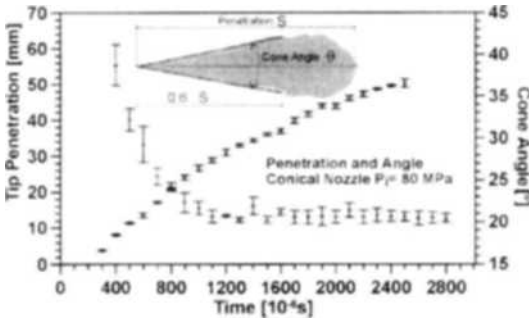


Fig. 5 Macroscopic parameters of the Spray. Mean values and the standard deviation for the conical nozzle, $P_i=80$ MPa

of 6 MPa, the variation range of CN varied between 2.3 for approximately 20 MPa, and 12.3 for approximately 80 MPa. The objective is then to establish if there is any change in the behavior of the spray in the cylindrical nozzle at the start of the cavitation for the pressure conditions that are close to the point determined numerically ($P_i=30$ MPa, $CN \approx 4$). In the case of the conical nozzle, this study serves to confirm that for this particular nozzle the changes in the macroscopic parameter are solely due to the changes in pressure conditions.

The macroscopic parameters of the spray that were characterized are the penetration (S) and the spray cone angle (θ). Both of these parameters on a generic spray are represented in Fig. 5. In the case of the spray angle, this is considered as the cone angle which is formed by the spray considering 60% of the penetration (Pastor et al., 2001). For example, in Fig. 5 the mean values and the standard deviation of penetration and cone angle are represented for the conical nozzle at the pressure $P_i=80$ MPa. As can be observed in the figure, the standard deviation is small in both cases: for the penetration the maximum standard deviation is around 0.7 mm. and for the cone angle is 1° . Therefore the error determining these macroscopic parameters is very small.

4.3.1 Influence of geometry on the spray tip penetration

The results in Fig. 6 show the evolution of

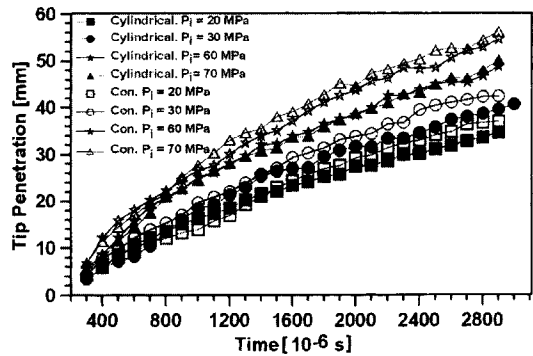


Fig. 6 Comparison of penetration between cylindrical and conical nozzle

the spray penetration for the conical and cylindrical nozzles. For simplification, the only curves shown are those that relate to the pressures $P_i=20$ MPa, $P_i=30$ MPa, $P_i=60$ MPa and $P_i=70$ MPa. As shown in Fig. 6, the penetration is related to the injection pressure increasing with it accordingly (Dent, 1971; Hay and Jones, 1972; Wakuri et al., 1960; Yeom, 2003).

On the other hand, if the penetration of both nozzles is compared, it can be observed that the penetration for the conical nozzle is, on average 10% higher than that of the cylindrical nozzle. This difference is wholly due to the geometrical differences between the two nozzles, showing the influence of the conicity and the rounding radii values on the penetration. These results are similar to the results of Blessing et al.(2003), in which the penetration of three nozzles with different grades of conicity are compared. Like these results, they concluded that the conicity of the nozzle increases the penetration and, as it will be seen in the following chapter, decreases the cone angle value.

At this point, it should be remembered that the value of the mean rounding radius for the conical nozzle is double that of the cylindrical nozzle, and the area reduction of the conical nozzle is 24% whilst the cylindrical nozzle has a value of just 3%. The conicity causes an increase in the exit velocity of the nozzle (Payri et al., 2002) and is therefore more responsible than the rounding radii for the increase of penetration, this being a factor that depends directly on the

velocity at the orifice exit.

4.3.2 Influence of geometry on the spray cone angle

Figure 7 shows the values of temporary evolution of the spray cone angle for the two nozzles, and as in the case of penetration, only four pressures are considered.

In the case of the cylindrical nozzle, the pressures of 60 MPa and 70 MPa show a cone angle which is higher than that for the pressures of 20 MPa and 30 MPa. In the case of the conical nozzle, the angle experiences a slight reduction with injection pressure.

Figure 8 shows the measured mean value of the semi-angle tangent of the spray for the cylindrical and conical nozzles, evaluated between the time spans of 1500 μ s and 3300 μ s, against the cavitation number CN, and for all the tested injection pressures. Only the instants higher than

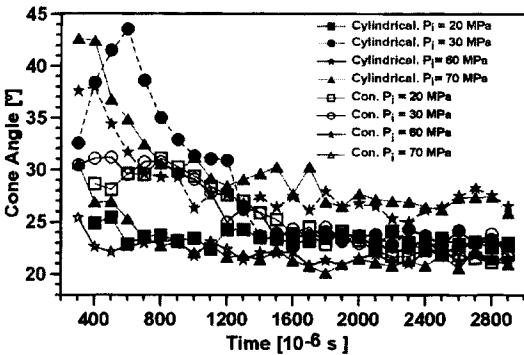


Fig. 7 Comparison of cone angle between cylindrical and conical nozzle

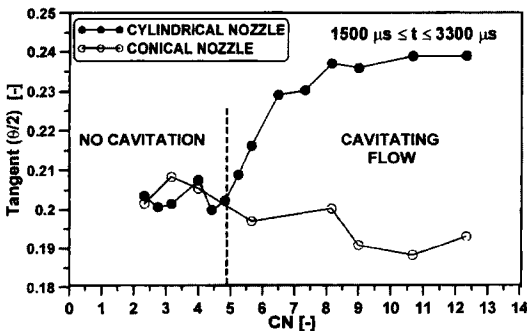


Fig. 8 Cone angle against the cavitation number

1500 μ s are considered, due to the fact that from this value the angle is relatively stable, following the first instants in which the measured angle value is less reliable owing to the small dimensions of the spray. As shown in Fig. 8, the semi-angle tangent and, therefore, the angle of the spray, experiences a considerable increase of approximately 15% for a CN value of 4.8, corresponding to an injection pressure of 35 MPa, which is slightly higher than the critical pressure obtained numerically ($P_i=30$ MPa, $CN_{crit}=4$).

This increase of the angle continues up to a pressure of 55 MPa ($CN=8.16$). According to the experiences of Chaves et al.(1995) the cavitation produces an increase in the spray angle right at the at the exact moment it begins, and this increases conforms with the most severe cavitation. At the point where cavitation extends to the outlet, known as super cavitation, the value of the angle is stabilized. In this case, the behavior shown by the spray is very similar to that observed by this author, that is to say that there is a clear zone where the spray is increasing, and afterwards a stabilization zone where the cavitation is assumed to be fully developed.

A difference appears between the value of CN_{crit} estimated with the CFD calculations, and the value of CN_{crit} for which an increase in the angle is observed. The value of CN that produces the start of the increase in the spray angle is a little higher than the value obtained from the CFD calculations, and therefore indicates a larger cavitation index in the case of the calculations.

A possible explanation of this difference may be related to the different treatment of the needle position in the calculations and in the experimental case. In fact, in the geometries simulated, the needle is considered when it is located at the maximum lift of 200 μ m. However, for the spray visualization tests, the injector functions under normal conditions with a pulse of 2 ms, therefore working with transitory lift and a lowering of the needle. Furthermore, even at the maximum lift the needle can suffer deformations due to the pressure difference between its ends, modifying the nominal geometry considered in the calcula-

tions. As evaluated by Macián et al. (2003b), the presence of the needle, mainly at low rises, affects the cavitation conditions, harnessing them and causing an increase in the critical cavitation number. This factor alone could justify the small differences found in the visualization tests and the numerical characterization concerned with the critical cavitation conditions.

In any case, the results are clear and significant: for cavitation numbers slightly higher than the critical cavitation number previously estimated, an increase takes place in the angle associated with the cavitation phenomenon. The differences found at the level of the critical cavitation number result because of the different test conditions that directly affect the critical cavitation conditions. From now on, for the following analysis, the critical cavitation number considered for the cylindrical nozzle will be the experimental ($CN_{crit}=4.8$ corresponding to $P_i=35$ MPa) at which the angle begins to increase because of cavitation.

The results for the conical nozzle shown in Fig. 8 do not show any significant variation in the behavior of the spray angle with the cavitation number. The general tendency in this case is a decrease in the semi-angle tangent with the injection pressure, which is linked to the convergent configuration of the orifices.

Comparing both types of nozzle, the conical nozzle shows measured values which are lower than those observed in the cylindrical nozzle, even in non-cavitating conditions. This is in concordance with the penetration results examined previously.

5. Analysis of the Results. Air-Fuel Mixture Prediction

The studies dedicated, at least principally, to the experimental or theoretical examination of free spray penetration are incredibly numerous (Dent, 1971 ; Hay and Jones, 1972 ; Wakuri et al., 1960). Many conclude with the proposal of an empirical or semi-empirical equation that tries to estimate the instant spray penetration related to diverse parameters (outlet velocity, environ-

ment density, orifice geometry ... etc). Hay and Jones (1972) carried out a critical revision of the proposed correlations in the bibliography for Diesel spray in the time period before 1972 and arrived at the conclusion that those which best fit the experimental results were the proposals by Wakuri et al. (1960) and Dent (1971). In this way, for example Wakuri et al. (1960) applying the conservation of the quantity of movement in a constant cone angle θ over a time period, where it is assumed that the air/fuel mixture is homogeneous, arrived at the equation, which according to Hay and Jones (1972) fits perfectly with the experimental data. Therefore as a reference in this study we take the expression proposed by them : (Wakuri et al., 1960)

$$S(t) = cte \cdot \Delta P^{1/4} \cdot \rho_a^{1/4} \cdot D_o^{1/2} \cdot \tan\left(\frac{\theta}{2}\right)^{-1/2} \cdot t^{1/2} \quad (3)$$

In this equation, $S(t)$ is the penetration in function of time, ρ_a is the air density, D_o is the diameter at the orifice outlet, ΔP is the pressure differential, t is the time from the start of injection and $\theta/2$ is the semi-angle of the spray cone. The geometry of the injector is taken into account through the diameter of the orifice and the value of the constant (cte).

The penetration behavior equation, which is established by the theory of gaseous sprays Eq. (3) can be written as :

$$S(t) = cte \cdot \rho_a^{-1/4} \cdot \dot{M}_o^{1/4} \cdot \tan\left(\frac{\theta}{2}\right)^{-1/2} \cdot t^{1/2} \quad (4)$$

where \dot{M}_o , is the momentum flux at the orifice outlet, equal to the mass flow rate times the velocity at the orifice outlet :

$$\dot{M}_o = \dot{m}_o \cdot U_o \quad (5)$$

by combining the Bernoulli equation and the mass conservation equation, the mass flow rate can be written as :

$$\dot{m}_o = C_a \cdot A_o \cdot \sqrt{2 \cdot \rho \cdot (P_i - P_b)} \quad (6)$$

The loss included in the discharge coefficient can be divided into two parts Eq. (7) : The velocity coefficient, C_v , takes into account the loss in velocity terms, and the area coefficient, C_a , which incorporates the loss of area due to the

flow contraction, the changes in density and the non-uniform velocity profiles at the hole outlet section (Desantes et al., 2003 ; Siebers, 1995):

$$C_d = C_a \cdot C_v \tag{7}$$

The velocity coefficient is defined, C_v , as the relationship between effective velocity and theoretical velocity:

$$C_v = \frac{U_o}{U_{th}} \tag{8}$$

Taking into account Eqs. (6) ~ (8), the Eq. (5) can be written as:

$$\dot{M} = \dot{m}_o \cdot U_o = \rho \cdot \frac{\pi}{4} \cdot D_o^2 \cdot C_v^2 \cdot C_a \cdot U_{th}^2 \tag{9}$$

Substituting Eq. (8) in Eq. (4):

$$S(t) = cte \cdot \left(\frac{\pi}{4} \cdot C_v^2 \cdot C_a \right)^{1/4} \cdot U_{th}^{1/2} \cdot D_o^{1/2} \cdot \left(\frac{\rho}{\rho_a} \right)^{1/4} \cdot \tan\left(\frac{\theta}{2}\right)^{-1/2} \cdot t^{1/2} \tag{10}$$

The term $D_o \cdot \left(\frac{\rho}{\rho_a} \right)^{1/2}$ is called equivalent diameter, D_{eq} .

Dividing both parts of Eq. (10) by the equivalent diameter gives the following expression for the non-dimensional penetration:

$$\frac{S(t)}{D_{eq}} = cte \cdot \left(\frac{\pi}{4} \cdot C_v^2 \cdot C_a \right)^{1/4} \cdot \left(\frac{U_{th} \cdot t}{D_{eq} \cdot \tan\left(\frac{\theta}{2}\right)} \right)^{1/2} \tag{11}$$

Shown in Fig. 9 is the representation of the penetration term of Eq. (11), opposed to the term raised to 1/2, for all the test points at different

pressures for the cylindrical nozzle.

Given that for this nozzle the non-cavitation, and cavitation zones have been clearly delimited, Fig. 9 represents the non-dimensional penetration for the two different pressure ranges: injection pressure less than 35 MPa (zone without cavitation), and pressures greater than 35 MPa (with cavitation). The linear adjustments and the corresponding equations for each of the zones are depicted in Fig. 9.

The represented points fit into in two straight lines. In fact, for the linear adjustments, the obtained level of correlation is 99, which indicates the almost total completion of the theoretical Eq. (11).

According to Eq. (12), the obtained slope of the straight line is the term:

$$cte \cdot \left(\frac{\pi}{4} \cdot C_v^2 \cdot C_a \right)^{1/4} \tag{12}$$

Or taking into account Eq. (7):

$$cte \cdot \left(\frac{\pi}{4} \cdot C_d \cdot C_v \right)^{1/4} \tag{13}$$

Differences can be appreciated between the slopes of the adjusted straight lines if the case without cavitation (1.227) is compared to the cavitating case for which the slopes of the lines are (1.243).

Comparing this term, for the cases with and without cavitation, Eq. (14) is formed for the cylindrical nozzle:

$$(C_d \cdot C_v)_{cavitating} / (C_d \cdot C_v)_{no\ cavitation} = 1.053 \tag{14}$$

which indicates an increase higher than 5% for the product of these two values in cavitating conditions with respect to conditions without cavitation. As established by the one-dimensional theory of cavitation proposed by Nurick (1976), which has been proved sufficiently in the bibliography (Macián et al., 2003b ; Schmidt and Corradini, 1997 ; Soteriou et al., 1995), once cavitation starts, the value of C_d decreases with the cavitation number according to Eq. (15):

$$C_d = C_c \cdot \sqrt{1 + \frac{1}{CN}} \tag{15}$$

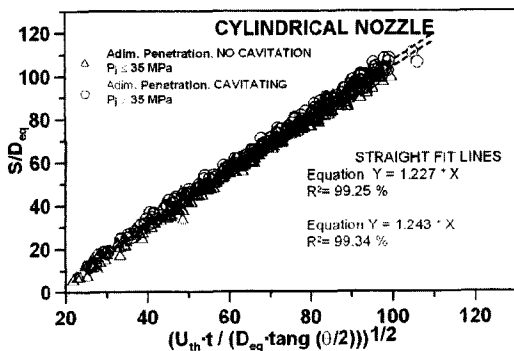


Fig. 9 Non-dimensional penetration for the cylindrical nozzle

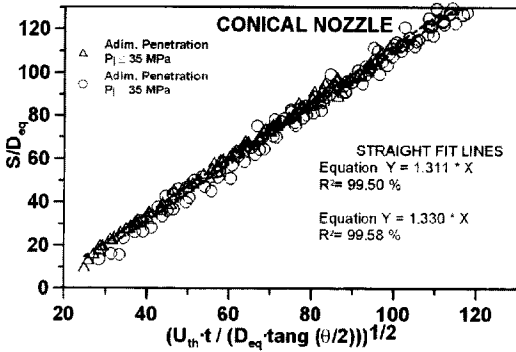


Fig. 10 Non-dimensional penetration for the conical nozzle

where C_c is the Nurick contraction coefficient.

Since in the cavitating conditions the value of C_d decreases, and taking into account Eq. (14), an important percentage increase in the value of C_v is noted. In cavitating conditions, and considering Eq. (7), a decrease in the contraction coefficient, C_a is observed. From this result, together with the angle increase, it can be deduced that the apparition of cavitation can substantially improve the air-fuel mixing process, due to the dependence of this phenomenon on both of these parameters.

Figure 10 proceeds in the same way with the conical nozzle, which represents non-dimensional penetration. In this case, even though cavitation does not occur, the results have been divided into two sections equal to those established for the cylindrical nozzle, thus obtaining two different adjustments in function of the low and high pressure intervals that correspond, as before, to the non-cavitation and cavitation zones in the cylindrical nozzle.

As in the cylindrical case, the value of the slopes of these straight lines represents the term shown in Eq. (7). In this case, the increase of this value with pressure is exclusively due to the increase in the coefficient $C_d \cdot C_v$, with injection pressure (Desantes et al., 2003).

6. Conclusions

From the present study several conclusions can be drawn :

(1) A precise geometrical determination of the nozzle used in this study has been made using a new technique based on the use of silicone moulds. Using this methodology it is possible to characterize diameters and the conicity level, which allow the reproduction of these geometries in order to be simulated using CFD calculations.

(2) CFD calculations have facilitated the investigation of the internal flow, as well as the detection of the critical cavitating conditions, arriving at the conclusion that the nozzle with lower level of conicity and smaller rounding radii cavitates. The nozzle with higher conicity and larger values of rounding radii does not cavitate even for high values of differential pressure.

(3) As far as the influence of the cavitation on the macroscopic behavior of the spray is concerned, it can be concluded that cavitation produces a considerable increase in the spray cone angle.

(4) By means of a theoretical analysis, with the limitations that this assumes, and combining the results of the macroscopic study of the spray together with previous works, it can be concluded that the cavitation is accompanied by an increase in the velocity coefficient, C_v and a decrease in the contraction coefficient, C_a .

(5) In non-cavitating conditions, for the conical nozzle, the small value of the spray angle observed is compensated by the increase in the value of the velocity coefficient. It is expected that the phenomenon of the preparation of the air-fuel mixture will be similar to that of the cylindrical nozzle.

(6) In developed cavitating conditions, the increase in the angle and in velocity coefficient, in the cylindrical nozzle, presumably leads to a better preparation of the mixture than with the conical nozzle.

Acknowledgment

The authors would like to thank Natalie Holmes* for helping to correct the English in this article and gratefully acknowledge the collaboration of Daniel Lerida*, Jose Enrique del Rey* and Carlos Perez* for providing the experimental

measurements.

(*) From CMT-Motores Termicos. Universidad Politecnica de Valencia.

References

Arcoumanis, C. and Gavaises, M., 1998, "Linking Nozzle Flow with Spray Characteristics in a Diesel Fuel Injection System," *Atomization and Sprays*, Vol. 8, pp. 307~347.

Arcoumanis, C., Flora, H., Gavaises, M., Kampanis, N. and Horrocks, R., 1999, "Investigation of Cavitation in a Vertical Multi-Hole Diesel Injector," *SAE Paper* 1999-01-0524.

Arcoumanis, C., Badami, M., Flora, H. and Gavaises, M., 2000, "Cavitation in Real-Size Multi-Hole Diesel Injector Nozzles," *SAE Paper* 2000-01-1249.

Badock, C., Wirth, R., Kampmann, S. and Tropea, C., 1997, "Fundamental Study of the Influence of Cavitation on the Internal Flow and Atomization of Diesel Sprays," *Proc. 13th ILASS-Europe 97*, Florence, July, 8-10, pp. 53~59.

Badock, C., Wirth, R. and Tropea C., 1999, "The Influence of Hydro-Grinding on Cavitation Inside a Diesel Injection Nozzle and Primary Break-Up Under Unsteady Pressure Conditions," *Proc. 15th ILASS-Europe 99*, Toulouse, July 5-7.

Bergwerk, W., 1959, "Flow pattern in Diesel Nozzle Spray Holes," *Proc. Inst. Mech. Engrs*, Vol. 173, No. 25.

Blessing, M., Konig, G., Kruger, C., Michels, U. and Schwarz, V., 2003, "Analysis of Flow and Cavitation Phenomena in Diesel Injection Nozzles and its Effects on Spray and Mixture Formation," *SAE Paper* 2003-01-1358.

Bunnell, R. A. and Heister, S. D., 2000, "Three-Dimensional Unsteady Simulation of Cavitating Flows in Injector Passages," *Journal of Fluids engineering (ASME)*, December, Vol. 122, pp. 791~797.

Chaves, H., Knapp, M. and Kubitzek, A., 1995, "Experimental Study of Cavitation in the Nozzle Hole of Diesel Injectors Using Transparent nozzles," *SAE Paper* 950290.

Choi, S. -H., Jeon, C. -H. and Chang Y. -J., 2002, "Steady-Flow Characteristics and its Influence on Spray for Direct Injection Diesel Engine," *KSME International Journal*, Vol. 61 No. 7, pp. 86~98.

Dent, J. C., 1971, "A Basis for Comparison of Various Experimental Methods for Studying Spray Penetration," *SAE Paper* 710571.

Desantes, J. M., Payri, R., Salvador, F. J. and Gimeno, J., 2003, "Measurements of Spray Momentum for the Study of Cavitation in Diesel Injection Nozzles," *SAE Paper* 2003-01-0703.

Flaig, U., Polach, W. and Ziegler, G., 1999, "Common Rail System for Passenger Car DI Diesel Engines; Experiences with Applications for Series Production Projects," *SAE Paper* 1999-01-0191.

Fluent Inc., 2001, "Fluent 6 User's guide,".

Ganippa, L. C., Bark, G., Andersson, S. and Chomiak, J., 2001, "Comparison of Cavitation Phenomenon in Transparent Scaled-Up Single-Hole Diesel Nozzles," *Proc. 4th International Symposium on Cavitation*, California Institute of Technology, Pasadena, CA USA, June 20-23.

Hay, P. and Jones, P. L., 1972, "Comparison of the Various Correlations for Spray Penetration," *SAE Paper* 720776.

He, L. and Ruiz, F., 1995, "Effect of Cavitation on Flow and Turbulence in Plain Orifices for High-Speed Atomization," *Atomization and Sprays*, Vol. 5, pp. 569~584.

Kampmann, S., Dittus, B., Mattes, P. and Kirner, M., 1996, "The Influence of Hydro-Grinding at VCO Nozzle on the Mixture Preparation in a DI Diesel Engine," *SAE Paper* 960867.

Koo, J. Y., 2003, "The Effects of Injector Nozzle Geometry and Operating Pressure Conditions on the Transient Fuel Spray Behavior," *KSME International Journal*, Vol. 17, No. 3, pp. 617~625.

Lee, J. H., Cho, S., Lee, S. Y. and Bae, C., 2002, "Development of Cavitation and Enhanced Injector Models for Diesel Fuel Injection System Simulation," *ImechE 2002, Proc Instn Mech Engrs* Vol. 216, Part D: J Automobile Engineering, pp. 607~618.

Macián, V., Bermudez, V., Payri, R. and Gimeno, J., 2003, "New Technique for the Determination of the Internal Geometry of Diesel Nozzle with the Use of the Silicone Methodology," *Experimental Techniques*, Vol. 27, No. 2, pp. 39~43.

Macián, V., Payri, R., Margot, X. and Salvador, F. J., 2003, "A CFD Analysis of the Influence of Diesel Nozzle Geometry on the Inception of Cavitation," *Atomization and Sprays*, Vol. 13, No. 5&6, pp. 579~604.

Nurick, W. H., 1976, "Orifice Cavitation and its Effects on Spray Mixing," *ASME J. Fluids Eng.*, pp. 681~687.

Ohrn, T. R., Senser, D. W. and Lefebvre, A. H., 1991, "Geometrical Effects on Discharge Coefficients for Plain-Orifice Atomizers," *Atomization and Sprays*, Vol. 1, No. 2, pp. 137~153.

Pastor, J. V., Arregle, J. and Palomares, A., 2001, "Diesel Spray Image Segmentation with a Likelihood Ratio test," *Applied Optics*, Vol. 40, No. 17, pp. 2876~2885.

Pastor, J. V., Payri, R., Lopez, J. J. and Julia, J. E., 2003, "Effect of Injector Nozzle Geometry of Diesel Engines on the Macroscopic Spray Characteristics by Means of Optical Techniques," Fuel Injection Systems. ImechE Conference Transactions. C610/014/2003, pp. 73~82.

Payri, R., Margot, X. and Salvador, F. J., 2002, "A Numerical Study of the Influence of Diesel Nozzle Geometry on the Inner Cavitating flow," *SAE Paper* 2002-01-0215.

Pierpont, D. A. and Reitz, R. D., 1995, "Effects of Injection Pressure and Nozzle Geometry on D.I. Diesel Emissions and Performance," *SAE*

Paper 950604.

Potz, C., Christ, W. and Dittus, E. B., 2000, "Diesel Nozzle the Determining Interface Between Injection System and Combustion Chamber," Thiesel 2000, Universidad Politecnica de Valencia, ISBN 84-7721-910-9.

Schmidt, D. P. and Corradini, M. L., 1997, "Analytical Prediction of the Exit Flow of Cavitating Orifices," *Atomization and Sprays*, Vol. 7, No. 6, pp. 603~616.

Schmidt, D. P., Rutland, C. J. and Corradini, M. L., 1999, "A Fully Compressible Two-Dimensional Model of High Speed Cavitating Nozzles," *Atomization and Sprays*, Vol. 9, pp. 255~276.

Siebers, D., 1995, "Scaling Liquid-Phase Penetration in Diesel Based on Mixing-Limited Vaporization," *SAE Paper* 950290.

Soteriou, C., Andrews, R. and Smith, M., 1995, "Direct Injection Diesel Sprays and the Effect of Cavitation and Hydraulic Flip on Atomization," *SAE Paper* 950080.

Versteeg, H. K. and Malalasekera, W., 1995, "An Introduction to Computational Fluid Dynamics. The finite volume method," Longman Scientific & Technical.

Wakuri, Y., Fujii, M., Amitani, T. and Tsunomeya, R., 1960, "Studies of the Penetration of a Fuel Spray in a Diesel Engine," *Bull. JSME*, Vol. 3, No. 9, pp. 123~130.

Yeom, J.-K., 2003, "A Study on the Behavior Characteristics of Diesel Spray by Using a High Pressure Injection System with Common Rail Apparatus," *KSME International Journal*, Vol. 17, No. 9, pp. 1371~1379.